Constraints on temperature–pressure conditions and fluid composition during metamorphism of the Sullivan orebody, Kimberley, British Columbia, from silicate–carbonate equilibria

Glen R. De Paoli and David R.M. Pattison

Abstract: The Sullivan mine, in southeastern British Columbia, is one of the world's largest sediment-hosted, massive sulphide deposits. It has undergone at least one period of metamorphism since it was deposited in mid-Proterozoic times. Mineral textures within the deposit are predominantly of metamorphic origin. A well-constrained estimate of metamorphic conditions is required to understand how the original, depositional character of the orebody has been modified by metamorphism. Metamorphic conditions were estimated using multiequilibrium thermobarometric techniques involving silicate–carbonate–fluid equilibria. Peak metamorphic temperature constrained by calibration of the garnet–biotite Fe–Mg exchange equilibrium is 450 ± 50°C. Lower temperature estimates from some samples are interpreted to record the temperature of cessation of garnet growth prior to the attainment of peak metamorphic temperature. Peak metamorphic pressure as determined from equilibria applicable to the assemblage garnet–biotite–muscovite–chlorite–calcite–quartz–fluid is 380 ± 100 MPa. The fluid composition accompanying this pressure estimate is $X_{H_2O} = 0.38$, $X_{CO_2} = 0.62 \pm 0.07$. This estimate is particular to one sample and may not be representative for the deposit as a whole. Metamorphic fluids at the estimated $P-T$ conditions would not have contained significant concentrations of C–O–H–S species other than H_2O and CO_2. Textural evidence and temperature–pressure results from a titanite-bearing metamorphosed mafic intrusion in the deposit suggest published titanite ages near 1330 Ma in the area of the mine represent the age of the peak metamorphic event. The results of this study carry tectonic implications for the Sullivan area, and may have application to other metamorphosed ore deposits and low-grade metamorphic settings.

Résumé : La mine Sullivan, dans le sud-est de la Colombie-Britannique, est un des plus gros gîtes du monde de sulfures massifs incorporés dans des sédiments. Il a subi au moins une crise métamorphique depuis sa formation du Protérozoïque moyen. Les textures des minéraux au sein du gîte sont principalement d'origine métamorphique. Une estimation cernant étroitement les conditions métamorphiques est nécessaire pour comprendre comment les caractères initiaux du dépôt de ce corps minéralisé ont été affectés par le métamorphisme. Les conditions métamorphiques ont été évaluées par les techniques thermobarométriques en équilibre multiple, impliquant les phases silicate–carbonate des fluides en équilibre. La température métamorphique culminante, contrainte par un étalonnage de l'échange en équilibre du Fe–Mg des minéraux grenat–biotite, est de 450 ± 50°C. Les estimations de température la plus basse de certains échantillons sont interprétées comme étant un enregistrement de la température de l'arrêt de croissance du grenat, avant que soit atteinte la température paroxysmique du métamorphisme. La pression métamorphique culminante, telle que déterminée à partir des conditions d'équilibre applicables à l'assemblage de grenat–biotite–muscovite–chlorite–calcite–quartz dans le fluide, est de 380 ± 100 MPa. La composition du fluide accompagnant cette estimation de la pression est $X_{H_2O} = 0{,}38$, $X_{CO_2} = 0{,}62 \pm 0{,}07$. Cette estimation étant particulière à un échantillon ne peut être représentative de tout le gîte. Les fluides métamorphiques aux conditions de $P-T$ estimées ne pouvaient contenir d'importantes concentrations des éléments C–O–H–S en dehors de H_2O et CO_2. Les observations texturales et les résultats obtenus pour la température–pression d'une intrusion mafique, métamorphisée,

Received February 25, 1995. Accepted July 19, 1995.

G.R. De Paoli and D.R.M. Pattison.[1] Department of Geology and Geophysics, The University of Calgary, Calgary, AB T2N 1N4, Canada.

[1] Corresponding author (e-mail: pattison@geo.ucalgary.ca).

métamorphisée, contenant de la titanite, et incorporée dans le gîte suggèrent que les âges publiés pour cette région, autour de 1330 Ma, représentent l'âge de l'évènement de la crise métamorphique culminante. Nos résultats révèlent des implications tectoniques pour la région de Sullivan, et il est possible de les appliquer à d'autres gîtes métallifères métamorphisés et à des contextes métamorphiques de degré faible.
[Traduit par la rédaction]

Introduction

The Sullivan mine near Kimberley, in southeastern British Columbia (Fig. 1), is one of the worlds largest lead–zinc orebodies (145×10^6 t) and is widely recognized as a classic example of a sedimentary-exhalative massive sulphide deposit (Ethier et al. 1976; Hamilton et al. 1982). The age of the orebody is approximately 1.4 Ga (LeCouter 1973) and it has experienced at least one period of metamorphism since then. Regional metamorphic grade in the vicinity of the orebody is greenschist facies (biotite–chlorite), with localized higher grade areas containing garnet and sillimanite (Fig. 1).

The Sullivan deposit has been the focus of a multidisciplinary study examining the genesis of giant sedimentary exhalative orebodies (Lydon et al. 1995). Before any interpretation of the original depositional character of the deposit can be made, the later effects of the metamorphic overprint must first be understood in order to separate metamorphic features from primary features. Characteristics of the deposit that will have been affected by metamorphism include the textures and mineralogy of the ore, gangue, and premetamorphic hydrothermal alteration zones; fluid inclusions; and stable isotopes. Economically, the metamorphic overprint has been of fundamental importance by recrystallizing and coarsening the sulphide minerals.

Previous estimates of the pressure–temperature ($P-T$) conditions of metamorphism at Sullivan have relied on a variety of sulphide equilibria and stable isotope fractionations (see below) and have produced equivocal results. The purpose of this study is to focus on the nonsulphide mineral assemblage and obtain internally consistent estimates of the metamorphic $P-T-$fluid conditions from silicate–carbonate–fluid equilibria using the TWEEQU software of Berman (1991). This technique has applications to other metamorphosed ore deposits. Complexities in the results carry implications for timing of equilibration and $P-T$ estimates in low-grade metamorphic rocks in general. With regard to the Sullivan deposit and its regional setting, the $P-T$ results of this study are different from previous estimates and carry implications for both the nature and timing of the metamorphic overprint and for the regional tectonic history.

Previous estimates of metamorphic conditions

Ethier et al. (1976) used a variety of methods to estimate metamorphic pressure and temperature for the Sullivan deposit. Temperatures between 400 and 560°C were obtained from oxygen-isotope fractionation between quartz and magnetite. Sulphur-isotope fractionation between sphalerite and galena gave a wide range of temperatures with a mean of 300 or 340°C, depending on which set of experimental data was used. Temperatures between 400 and 490°C were obtained from the arsenopyrite geothermometer of Kretschmar and Scott (1976), and a pressure of 500 MPa was obtained from the sphalerite geobarometer of Scott (1973). The temperature estimate determined from the arsenopyrite geothermometer should be considered approximate, as the experimental curve of Kretschmar and Scott (1976) is not well constrained. Ethier et al. (1976) noted that the 500 MPa estimate is well in excess of what can be accounted for stratigraphically (maximum of 7600 m, or 200 MPa), and cautioned that reequilibration between sphalerite and pyrrhotite during cooling from peak metamorphic conditions may have been responsible for the anomalously high pressure estimate.

Leitch (1991) and Leitch and Turner (1992) determined average homogenization temperatures of 200–415°C for low-salinity fluid inclusions of possible metamorphic origin from the Sullivan deposit. However, correcting these temperatures to 200 MPa gives approximately 500–675°C (Leitch 1991), inconsistent with the garnet–biotite–chlorite assemblage in the deposit. The inclusions are found in enigmatic quartz (±calcite) "clasts" in milled sulphides, which may be broken vein fragments (C.H.B. Leitch, personal communication, 1994).

Petrography

Samples were classified into three rock types: silicate matrix rocks, sulphide matrix rocks, and an amphibolite unit. Mineral textures are clearly metamorphic in origin (Fig. 2), although the samples examined show little to no foliation.

The silicate matrix rock type includes samples from the waste beds (sulphide-poor clastic interbeds) within the bedded ore. The overall mineral assemblage is Qtz + Ms + Bt ± Chl ± Grt ± Pl ± Cal (abbreviations after Kretz 1983) with minor amounts of pyrrhotite, sphalerite, galena, and pyrite. The matrix is composed of roughly equal amounts of fine-grained (10–50 μm) quartz and muscovite. In some samples, biotite and chlorite are fine grained enough to be considered matrix as well. Plagioclase (possibly peristerite, see Mineral chemistry section) was identified in the matrix of some of the samples. Garnet porphyroblasts are found in most samples. They range from 0.1 to 1.0 mm in diameter, and occur as isolated idiomorphic grains, with inclusion-rich cores (Fig. 2*a*), and as aggregates of poikiloblastic grains rimming pyrrhotite laths. Garnet inclusions include quartz, calcite, chlorite, and pyrrhotite. Biotite and chlorite porphyroblasts occur as randomly oriented idiomorphic grains up to 1.0 mm. Calcite is rare in this rock; where found, it ranges from matrix size to 0.5 mm. The larger calcite grains are subidiomorphic and tend to form aggregates, often rimming pyrrhotite laths. Sulphide minerals make up $< 10\%$ of this rock type. Pyrrhotite is the most common sulphide, occurring as idiomorphic lath-shaped grains averaging

0.2 mm. Accessory minerals include apatite, titanite, and zircon.

The sulphide matrix rock type includes samples from the sulphide-rich layers in the bedded ore. The overall assemblage is variable, typically Po ± Sp ± Gn ± Py with Qtz ± Ms ± Cal ± Grt ± Bt ± Chl. The matrix is >50% sulphide minerals, including pyrrhotite, sphalerite, galena (±boulangerite), and pyrite. Grain size averages 0.10–0.25 mm. The textures of the sulphide minerals show the following variations: anhedral equigranular pyrrhotite, galena, and sphalerite; massive pyrrhotite or sphalerite containing small anhedral blebs of sphalerite, pyrrhotite, or galena; and a crudely banded texture of pyrrhotite, sphalerite, and galena. Nonsulphide minerals in the matrix include subidiomorphic to anhedral quartz and carbonate, and subidiomorphic to idiomorphic garnet, muscovite, biotite, and chlorite. Carbonate is much more abundant than in the silicate lithology. Idiomorphic garnet, biotite, muscovite, and chlorite porphyroblasts reach 2 mm in diameter. Garnet-rich laminae are often found at the contact with silicate layers (Fig. 2*b*). Overall, silicate mineral grain size in the sulphide matrix rocks is larger than in the silicate matrix rocks.

The amphibolite unit is represented by sample S-15 from the "gabbro arch," a metamorphosed body of the Moyie suite of gabbro and diorite intrusions that cuts through the western edge of the deposit. Metamorphic minerals and textures in this sample have largely obliterated the original igneous character. The rock is composed of equigranular, subidiomorphic to idiomorphic amphibole, chlorite, quartz, plagioclase, clinozoisite, and calcite (Fig. 2*c*). Plagioclase shows complex textures and is severely sericitized. Pyrrhotite and ilmenite are disseminated throughout. Ilmenite is nearly always rimmed by titanite and (or) clinozoisite (Fig. 2*d*).

Mineral chemistry

Data collection

Thirteen samples were selected for microprobe analysis (De Paoli 1994). Mineral phases were analyzed using the ARL SEMQ 9-channel wavelength-dispersive electron microprobe at the University of Calgary. Silicate minerals were analyzed with an operating voltage of 15 keV, a beam current of 0.15 μA, a beam diameter of 1 μm, and a counting time of 20 s. For carbonate minerals a beam current of 0.10 μA and a beam diameter of 3.0 μm were used to minimize devolatization (see Nicholls et. al 1977 for data reduction methods).

Selected compositional data for garnet and biotite rim analyses (mole fractions) are given in Table 1.[2] The data in Table 1 represent the average of at least five analyses. Analysis point selection is described in the $P-T-X$ estimate, Method section. Analyses from sample S3-11 (location 2, see below) are given in Table 2. Analyses from sample S-15 are given in Table 3.

Mineral composition variations

In many metamorphosed ore deposits, silicate minerals such as garnet, biotite, and chlorite are more Mg rich and less Fe rich in sulphide-rich rocks than in sulphide-poor ones (Froese 1969; Bachinski 1976; Hutcheon 1979; Nesbitt 1982). Within the Sullivan deposit, differences in mineral compositions between the silicate and sulphide rock types are noticeable, but two distinct populations of Fe/(Fe + Mg) ratios cannot be discerned. As an example, Fig. 3 shows Fe/(Fe + Mg) versus X_{Sps} in garnet rims for both the silicate and sulphide lithologies (analyses given in Table 1). Although the range of Fe/(Fe + Mg) ratios in garnets in the sulphide lithology is slightly lower (from 0.888 to 0.953) than in the silicate lithology (from 0.904 to 0.963), and the range of manganese content in garnets in the sulphide lithology is slightly higher (from 0.277 to 0.518 X_{Sps}) than in the silicate lithology (0.09 to 0.454 X_{Sps}), there is significant overlap in the range of values between the two rock types. The figure also shows that in both rock types, garnets with higher X_{Sps} have lower Fe/(Fe + Mg). Garnet core analyses show a similar trend in Fe/(Fe + Mg) and X_{Sps}.

Biotite compositions in the same samples show a similar trend. The range of Fe/(Fe + Mg) in biotite in the sulphide lithology is lower (0.315–0.596) than that in a silicate

Fig. 1. Simplified geological map of the Sullivan mine region. Compiled from Lis and Price (1976), Benvenuto and Price (1979), McMechan and Price (1982), and Read et al. (1991).

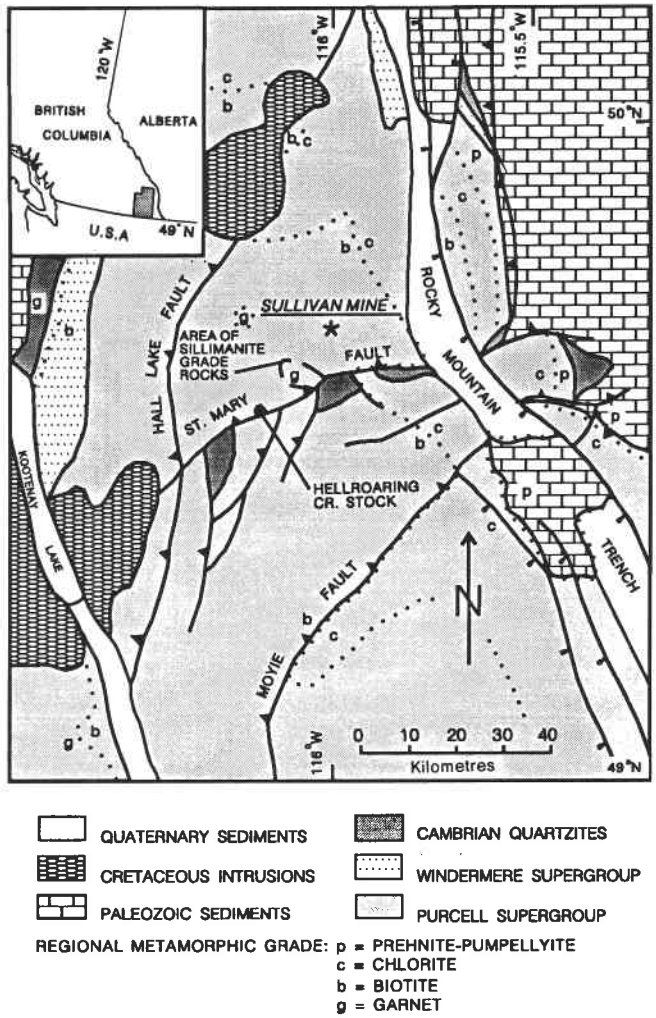

[2] Full analyses of minerals in Table 1 may be purchased from the Depository of Unpublished Data, CISTI, National Research Council Canada, Ottawa, ON K1A 0S2, Canada.

Fig. 2. Photomicrographs of typical mineral textures in the Sullivan orebody. (*a*) Sample S3-11 from a waste band within the bedded ore showing garnet (Grt) and calcite (Cal), along with randomly oriented sheet silicate minerals (Ms, muscovite; Bt, bitotite; Chl, chlorite). (*b*) Sample S3-18, contact between silicate waste layer (left side) and sulphide layer (right side) within bedded ore showing larger garnets in the sulphide layer. (*c*) Sample S-15 from the metamorphosed mafic intrusion. SP, sericitized plagioclase. (*d*) Sample S-15 showing titanite (Ttn) rimming ilmenite.

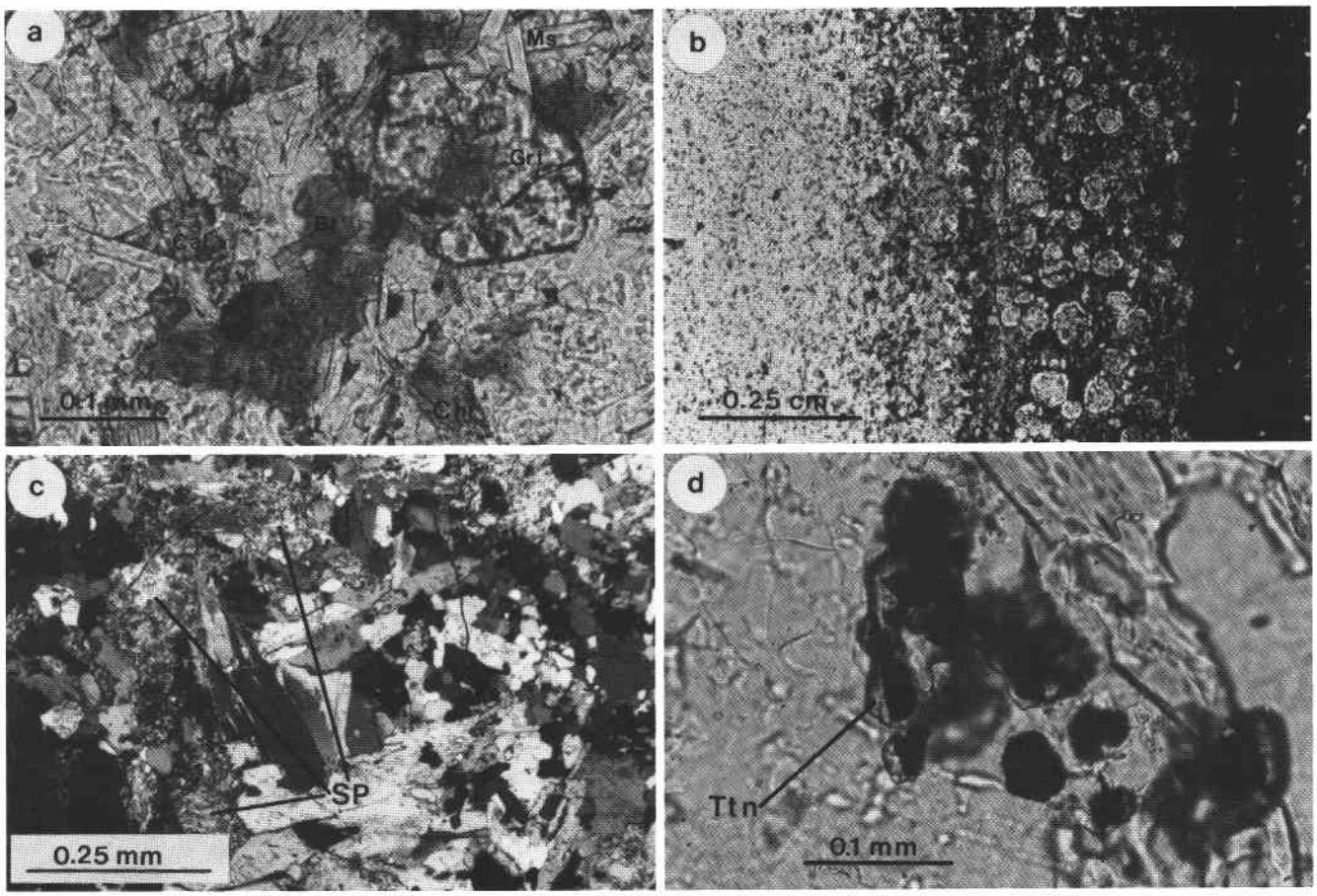

Table 1. Selected garnet–biotite compositional data and temperatures at 400 MPa for the Berman (1990) calibration of the garnet–biotite Fe–Mg exchange geothermometer.

Sample No.	Lithology[a]	Garnet[b]					Biotite[c]					Mode % Chl[d]	T (°C)
		X_{Fe}	X_{Mg}	X_{Mn}	X_{Ca}	Fe/(Fe + Mg)	X_{Fe}	X_{Mg}	$X_{Al^{VI}}$	X_{Ti}	Fe/(Fe + Mg)		
S1-57	Silicate	0.359	0.038	0.454	0.138	0.904	0.334	0.514	0.103	0.033	0.394	Trace	377
S3-11	Silicate	0.726	0.031	0.143	0.100	0.959	0.598	0.267	0.095	0.032	0.691	5	460
S3-14	Sulphide	0.338	0.038	0.518	0.106	0.899	0.284	0.617	0.061	0.022	0.315	—	296
S3-16	Silicate	0.723	0.028	0.219	0.024	0.963	0.590	0.256	0.112	0.025	0.697	—	411
S3-18	Sulphide	0.666	0.033	0.277	0.017	0.953	0.518	0.351	0.080	0.041	0.596	15	364
S3-22	Silicate	0.609	0.031	0.320	0.037	0.952	0.497	0.356	0.107	0.027	0.583	—	365
S7-150	Silicate	0.566	0.043	0.337	0.040	0.929	0.504	0.350	0.092	0.039	0.590	20	451
S7-153	Silicate	0.610	0.055	0.294	0.034	0.917	0.464	0.393	0.098	0.031	0.541	5	448
S7-155	Silicate	0.604	0.050	0.277	0.057	0.924	0.441	0.413	0.102	0.028	0.516	Trace	416
DS-47	Silicate	0.752	0.036	0.123	0.084	0.954	0.551	0.303	0.105	0.036	0.645	40	431
DS-85	Silicate	0.783	0.036	0.090	0.084	0.956	0.572	0.273	0.117	0.032	0.677	40	456
UCG-84	Sulphide	0.427	0.054	0.476	0.036	0.888	0.341	0.531	0.092	0.021	0.391	—	385

Notes: Data are for rim analyses.

[a]Indicates whether matrix is predominantly silicate or sulphide minerals.

[b]$X_i = i/(Fe + Mg + Mn + Ca)$.

[c]$X_i = i/(Fe + Mg + Mn + Al^{VI} + Ti)$.

[d]By visual estimation.

Table 2. Average mineral analyses from location 2, sample S3-11.

	Grt (n = 11)	Bt (n = 8)	Ms (n = 12)	Chl (n = 6)	Cal (n = 6)
SiO_2 (wt.%)	39.95	33.86	46.38	23.41	0.08
TiO_2	<0.02	1.54	0.20	0.02	na
Al_2O_3	20.90	17.66	34.99	20.93	0.04
FeO	32.06	26.93	1.75	34.74	0.76
MnO	6.25	0.43	na	0.35	1.50
MgO	0.76	6.74	0.68	8.90	0.14
CaO	3.42	0.07	0.02	<0.01	53.97
Na_2O	na	<0.03	0.6	<0.03	na
K_2O	na	8.21	10.87	<0.01	na
F	na	0.06	0.17	<0.08	na
H_2O	na	3.53	4.42	10.83	43.90[a]
Total	100.38	99.33	100.00	99.18	100.40
Si (ppm)	3.008	5.302	6.176	5.182	—
Ai^{IV}	—	2.698	1.824	2.818	—
Ti	—	0.180	0.020	0.004	—
Al^{VI}	1.987	0.562	3.670	2.646	—
Fe	2.178	3.526	0.194	6.432	0.011
Mn	0.430	0.058	—	0.064	0.021
Mg	0.093	1.574	0.134	2.938	0.003
Ca	0.298	0.012	0.002	—	0.964
Na	—	—	0.158	—	—
K	—	1.640	1.846	—	—
Sum	7.998	15.552	14.024	20.084	0.999
F	—	0.310	0.070	—	—
OH	—	3.690	3.861	16.000	0.999[b]

Notes: Data are for rim analyses. na, not analyzed. See Nicholls et al. (1977) for data reduction methods. Cations based on garnet = 12O, biotite = 24(O, OH, F), muscovite = 24(O, OH, F), chlorite = 18(O, OH, F), and calcite = 3O. H_2O and CO_2 from stoichiometry. All Fe assumed to be Fe^{2+}.

[a] CO_2.

[b] C.

matrix (0.396−0.697), but the overlap is large. Biotite in a sulphide matrix tends to be more Si rich and Al poor than in a silicate matrix (see Table 2).

Plagioclase compositions in the deposit vary widely, and likely represent some or all of relict detrital grains, albite related to premetamorphic hydrothermal alteration, and peristerite. Fine-grained (50 μm) plagioclase crystals were identified with the electron microprobe in the matrix of sample S7-153. Compositions range from pure albite to An_{28} (78 analyses), with a gap from An_3 to An_{13} (with one value of An_7). The virtual absence of analyses between An_3 and An_{13} suggests the feldspar in this sample may be peristerite. However, at 450°C and 380 MPa (the preferred $P-T$ estimate of metamorphism, see below), the peristerite gap spans approximately An_3 to An_{20}, not An_3 to An_{13}, and oligoclase compositions are expected to be $>An_{20}$, not $>An_{13}$ (Maruyama et al. 1982). Sample S4-6 contains large (0.1 mm), oval-shaped plagioclase grains with an anorthite content of An_{37} to An_{40}, having irregular-shaped overgrowths of composition An_0 to An_{28} (with no compositional gap). The shape and high anorthite suggest these are relict detrital grains. The overgrowths may be a complex intergrowth of premetamorphic albite and peristerite. Efforts to image textures of individual plagioclase grains in the above two samples using the scanning electron microscope were unsuccessful.

Similar attempts to determine composition−textural relationships for plagioclase in sample S-15 from the amphibolite unit also yielded equivocal results, and were further complicated by the strongly sericitized nature of the grains. In sample S-15, plagioclase compositions range from pure albite to An_{17}, with no compositional gap.

P−T−X estimate

The garnet−biotite Fe−Mg exchange equilibrium was used for temperature estimation. One sample with the mineral assemblage Grt−Bt−Ms−Chl−Cal−Qtz provided constraints on the pressure and metamorphic fluid composition. Titanite textures and $P-T-X$ results from a sample of the metamorphosed mafic intrusion carry implications for the age of metamorphism.

Method

For the temperature estimation, touching garnet and biotite rims (within 10 μm of the rim) were selected. The pressure

Table 3. Average mineral analyses for sample S-15.

	Amp (n = 11)	Ep (n = 9)	Chl (n = 15)	Ttn (n = 15)	Ilm (n = 12)	Cal (n = 9)
SiO_2 (wt.%)	46.45	39.06	26.12	31.86	0.09	<0.04
TiO_2	0.30	0.04	0.02	38.63	52.01	na
Al_2O_3	11.61	27.59	20.76	1.48	0.04	<0.04
FeO	16.13	na	24.73	na	42.71	0.71
Fe_2O_3	na	7.55	na	0.77	0.711	na
MnO	0.26	0.10	0.25	0.07	4.20	0.52
MgO	10.37	0.13	16.57	0.06	0.16	0.32
CaO	11.93	23.69	0.02	26.90	0.24	54.14
Na_2O	1.01	na	na	na	na	na
K_2O	0.16	na	<0.01	na	na	na
F	0.08	0.02	<0.08	0.26	na	na
H_2O	1.97	1.92	11.53	1.06	na	43.59[a]
Total	100.25	100.10	100.02	101.00	100.17	99.28
Si (ppm)	6.808	3.030	5.183	1.018	0.005	—
Al^{IV}	1.192	—	2.275	—	0.003	—
Ti	0.033	0.003	0.003	0.918	1.980	—
Al^{VI}	0.815	2.522	2.817	0.055	—	—
Fe^{2+}	1.978	—	4.303	—	1.800	0.010
Fe^{3+}	—	0.441	—	0.009	0.027	—
Mn	0.032	0.007	0.044	0.002	0.180	0.007
Mg	2.264	0.015	5.137	0.003	0.012	0.008
Ca	1.874	1.969	0.004	0.911	0.013	0.975
Na	0.288	—	—	—	—	—
K	0.030	—	—	—	—	—
Sum	15.314	7.987	20.017	2.916	4.020	1.000
F	0.036	0.006	—	0.103	—	—
OH	1.964	0.994	16.000	0.897	—	1.000[b]

Notes: Data are for rim analyses. na, not analyzed. See Nicholls et al. (1977) for electron microprobe operating conditions and reduction methods. Cations based on amphibole = 24(O, OH, F), epidote = 13(O, OH, F), chlorite = 18(O, OH, F), titanite = 5(O, OH, F), ilmenite = 6O, and calcite = 3O. For amphibole, chlorite, and calcite, all Fe is assumed to be Fe^{2+}. For epidote and titanite, all Fe is assumed to be Fe^{3+}. Fe^{3+} in ilmenite = Fe − (2 − (Mn + Mg + Ca)) iterated. H_2O and CO_2 from stoichiometry. Amp, amphibole.

[a] CO_2.

[b] C.

and fluid composition estimate in sample S3-11 required analyses of garnet, biotite, muscovite, chlorite, and calcite (quartz was assumed to be pure). To perform thermobarometric calculations for this sample, the assumption must be made that all analyzed portions of the five phases of interest equilibrated during prograde metamorphism and did not subsequently change during cooling. The volume of the sample within which this criterion is satisfied, the equilibrium volume, may be expected to be relatively small in low-grade rocks such as those at the Sullivan deposit. The size of the equilibrium volume in a given rock is a function primarily of temperature, intergranular fluid mobility, grain size, compositional homogeneity, and the duration of the metamorphic event. In sample S3-11, three small areas were selected, within which all five minerals were in close proximity. At each location, touching garnet and biotite rims were selected for analysis, along with the rims of the other minerals closest to the garnet–biotite pairs. The maximum diameter of the area required to include all phases of interest was 2 mm. To evaluate the equilibrium volume for this sample, biotite isolated from garnet, and biotite immediately inside the diameter of the area required to include all phases was also analyzed. In all three locations, the compositions of isolated biotite and biotite in contact with garnet are within one standard deviation of each other and show no consistent spatial pattern. This result is consistent with the assumption that the diameter of the area that includes all phases of interest at each of the three locations probably does not exceed the diameter of the equilibrium volume of this sample, and that all analyzed phases were likely in chemical equilibrium.

Each of the three locations in sample S3-11 was treated as a separate chemical system, and the $P-T-X_{CO_2}$ determination for each location was averaged to determine the $P-T-X_{CO_2}$ estimate for the sample as a whole. This approach accounts for small-scale variations in bulk composition within the sample.

All thermobarometric calculations were made using the program TWEEQU, version 1.02 (Berman 1988, 1991). Activity models used are shown in Table 4. Daphnite (Fe-chlorite) was not used in any of the calculations, because

temperatures from the garnet–chlorite Fe–Mg exchange equilibrium for both the El-Shazly and Liou (1991) and the Symmes and Ferry (1992) thermodynamic data for daphnite were consistently found to be 50–150°C higher than garnet–biotite Fe–Mg exchange equilibrium temperatures from the same sample.

Geothermometry

The Berman (1990) calibration of the garnet–biotite Fe–Mg exchange equilibrium was used to estimate peak metamorphic temperature in this study. It was chosen because (*i*) it is the only fluid-independent, temperature-sensitive equilibrium for which the required assemblage was available; (*ii*) it is based on a thorough assessment of high-quality experimental data; and (*iii*) use of TWEEQU computer software (Berman 1988, 1991) for pressure–fluid composition estimates requires the calibration to maintain the internal consistency of the data base.

Table 1 shows selected garnet and biotite analyses and the temperature estimates from 12 samples. There is a wide range of garnet and biotite compositions and temperatures (296–460°C) between the samples. Possible explanations for the large range of temperature estimates include (*i*) the analyzed portions of the minerals were not in chemical equilibrium; (*ii*) peak metamorphic temperature varied within the deposit; (*iii*) variable resetting of Fe–Mg distribution between garnet and biotite occurred during cooling; (*iv*) nonideal mixing (particularly Mn in garnet) may have caused systematic displacement of the equilibrium; and (*v*) Fe–Mg fractionation between garnet and biotite ceased at different temperatures in different samples. Below, we address each of these possibilities in turn.

(*i*) The identical analytical approach was used for all samples. Touching garnet and biotite rims were analyzed to reduce the possibility of selecting compositions that were not in chemical equilibrium at peak metamorphic temperature. Close similarity of compositions from numerous Grt–Bt pairs in individual samples was consistent with attainment of equilibrium.

(*ii*) Given the relatively small size of the deposit (diameter 2 km) relative to variation in regional metamorphic grade (Fig. 1), significant variations in temperature within the Sullivan orebody are not expected. Temperature estimates from samples in close proximity to one another can vary substantially, indicating a cause other than a regional phenomenon. For example, sample S3-11 yields a temperature estimate of 460°C, whereas sample S3-14, only a few metres away from S3-11, yields a temperature estimate of 296°C. There is no indication of significant contact-metamorphic effects associated with the mafic intrusion known as the gabbro arch in the western part of the deposit (Cominco geologists, personal communication, 1992). Supporting this view is the absence of any systematic increase in temperature estimate for those samples closer to the intrusion. The intrusion is itself metamorphosed to greenschist facies, and was therefore probably emplaced prior to the peak metamorphic event.

(*iii*) Resetting of Fe–Mg distribution between garnet and biotite during cooling appears unlikely. Diffusion rate calculations (e.g., Spear 1991) indicate that cation diffusion rates in garnet at temperatures below 450°C are negligible for any reasonable time scales. This would effectively prevent any change in garnet composition during cooling. Possible Fe–Mg reequilibration between biotite, chlorite, and sulphides following closure of garnet is unlikely owing to negligible variations in Bt and Chl compositions at different locations in individual samples, and the absence of significant core–rim variations in these minerals. Consequently, garnet–biotite Fe–Mg fractionations are likely to have been preserved from prograde conditions.

Fig. 3. Fe/(Fe + Mg) vs. X_{Sps} in garnet. Rim analyses plotted. Although garnets in a sulphide matrix tend to have lower Fe/(Fe + Mg) and higher X_{Sps} than in a silicate matrix, the broad range of compositions from both rock types overlap significantly. Garnets with higher X_{Sps} have lower Fe/(Fe + Mg) in both rock types.

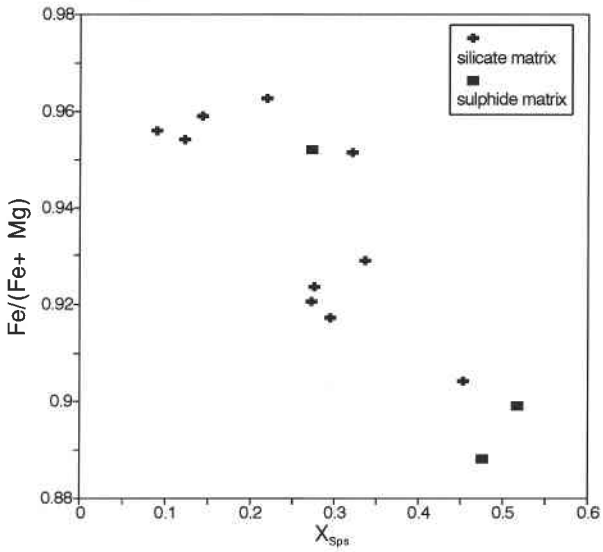

(*iv*) A plot of temperature versus X_{Sps} in garnet (Fig. 4) shows lower temperature estimates tend to come from samples with higher manganese content. This is the expected trend if nonideal Mn mixing in garnet was significant (the Berman (1990) calibration assumes manganese mixes ideally). No experimental data exist for Mn mixing in garnet at greenschist–amphibolite conditions, so nonideal behavior cannot be completely discounted. However, many empirical studies (e.g., Hodges and Spear 1982; Chipera and Perkins 1988; Raeside et al. 1988) support ideal Mn mixing in garnet. Raeside et al.'s (1988) study is especially important in this regard, because low-grade garnets in their study were relatively Mn rich (e.g., X_{Mn} = 0.381, T = 304°C), and their low temperature estimates fit well in a prograde sequence (contact aureole).

(*v*) A possible explanation for the range in temperature estimates is that Fe–Mg fractionation between garnet and biotite ceased prior to the attainment of peak metamorphic temperature in some samples. This situation might occur if garnet growth stopped in these samples before peak metamorphic temperatures were reached. Because diffusion rates in garnet below 450°C are believed to be negligible (Spear 1991), any change in Fe–Mg fractionation between garnet and biotite, induced either by an increase or decrease in temperature, might only be recorded during periods of garnet and biotite recrystallization. Walther and Wood (1984) noted that mass transfer during prograde metamorphism is

Table 4. Activity models used in thermobarometric calculations.

Mineral	End member	Activity model	Reliability[a]
Garnet	Almandine	Berman 1990	1
Garnet	Grossular	Berman 1990	1
Garnet	Pyrope	Berman 1990	1
Biotite	Annite	McMullin et al. 1991	3
Biotite	Phlogopite	McMullin et al. 1991	1
White mica	Muscovite	Chatterjee and Froese 1975	1
Amphibole	Tremolite	Mader and Berman 1992	2
Amphibole	Actinolite	Mader and Berman 1992	3
Chlorite	Clinochlore	Begin 1992	2
Epidote	Clinozoisite	Droop 1985	3
Titanite	—	Ideal	1
Ilmenite	—	Ideal	1
Calcite	—	Ideal	1
Quartz	—	Ideal	1

[a]Reliability of thermodynamic data from Berman (1991).

Fig. 4. Temperature at 400 MPa vs. X_{Sps} in garnet using rim analyses. Temperatures from the Berman (1990) calibration of the garnet–biotite Fe–Mg exchange geothermometer. See Table 1 for garnet–biotite compositional data. The figure shows lower temperature estimates from samples with higher X_{Sps} in garnet.

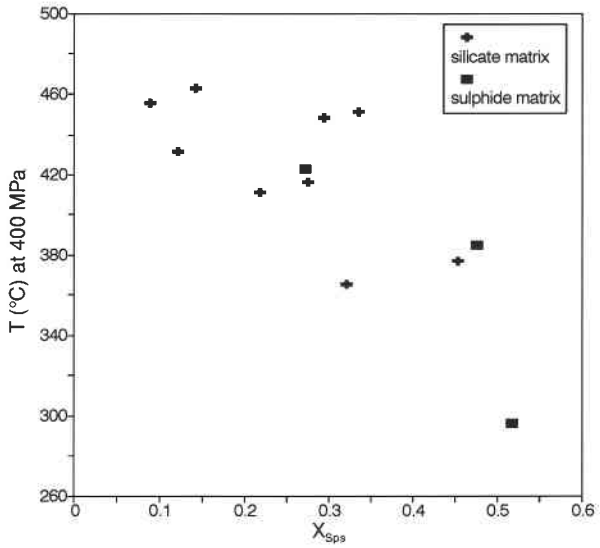

achieved predominantly through the progress of devolatization reactions via a solution and precipitation mechanism in the presence of an intergranular fluid. This view is based on experimental data indicating that rates of solution–precipitation in the presence of a fluid (Wood and Walther 1983) are orders of magnitude faster than volume diffusion, for example Fe–Mg interdiffusion in garnet (Chakraborty and Ganguly 1991).

Some garnets may have stopped growing earlier than others due to the loss of a reactant phase involved in garnet growth, in particular, the phase or phases supplying manganese. Manganese is a significant component of many garnets in the deposit (up to 37 wt.% MnO), and manganese has been shown to stabilize garnet at lower temperatures than in a pure Fe–Mg system (Symmes and Ferry 1992). Figure 1 shows garnet is not part of the regional metamorphic assemblage in the vicinity of the Sullivan mine. Consequently, the most likely explanation for the abundance of garnet within the orebody is an unusually Mn-rich bulk-rock composition.

Several reactant phases may have supplied manganese to the garnets in the deposit. The high manganese content and high modal abundance of garnet in many samples, sulphide-matrix samples in particular (e.g., 37 wt.% MnO and 85 mode % garnet in one sample), require a very Mn-rich reactant phase, such as rhodochrosite ($MnCO_3$) or pyrolusite (MnO_2). Pyrolusite is unlikely to have been present in the deposit at the time of deposition, because of reducing conditions in the sedimentary basin (W. Goodfellow, personal communication, 1995). Reactions involving rhodochrosite and detrital clay minerals may have produced Mn-rich garnet by a reaction of the type

$$[1]\quad 3MnCO_3 + Al_2Si_2O_5(OH)_4 + SiO_2 = Mn_3Al_2Si_3O_{12} + 3CO_2 + 2H_2O$$

Although no rhodochrosite or other Mn-rich minerals have been reported from the Sullivan deposit, they may have been part of the original mineralogy of the deposit at the time of its deposition. The most Mn-rich minerals found in this study, aside from garnet, are carbonate (up to 4.58 wt.% MnO), chlorite (up to 1.14 wt.% MnO), and to a lesser degree, sulphide minerals (sphalerite, up to 0.45 wt.% MnO; pyrrhotite, up to 0.22 wt.% Mn; Campbell and Ethier 1983), any of which may have been subordinate sources of manganese.

Petrographic evidence indicates that chlorite may also have been an important reactant phase during garnet growth. Those samples which give low temperature estimates (<430°C) contain no chlorite or trace chlorite, whereas samples giving higher temperature estimates (>430°C, including all five samples selected for the temperature estimate, see below) contain significant (5–40%) chlorite (see Table 1). Garnet may have grown via a chlorite-consuming reaction of the type

$$[2]\quad \text{chlorite(Mn)} + \text{muscovite} + \text{quartz} = \text{garnet(Mn)} + \text{biotite} + H_2O$$

and ceased at the temperature at which the chlorite was

Fig. 5. (*a*) Pressure–temperature, (*b*) pressure–X_{CO_2}, and (*c*) temperature–X_{CO_2} diagrams for location 2, sample S3-11. Mineral assemblage is Grt–Bt–Ms–Chl–Cal–Qtz. Three independent equilibria. Intersection temperature = 460°C; pressure = 360 MPa; X_{H_2O} = 0.38. Equilibria are as follows (Cln = clinochlore): 1, Alm + Phl = Prp + Ann; 2, 4Ann + 3Cln + Ms + 3Qtz = 4Alm + 5Phl + $12H_2O$; 3, Alm + 3Cln + Ms + 3Qtz = 5Prp + Ann + $12H_2O$; 4, 3Cln + Ms + 3Qtz = 4Prp + Phl + $12H_2O$; 5, Alm + Ms + 6Cal + 3Qtz = 2Grs + Ann + $6CO_2$; 6, Prp + Ms + 6Cal + 3Qtz = 2Grs + Phl + $6CO_2$; 7, 2Grs + 5Ann + 3Cln + $6CO_2$ = 5Alm + 5Phl + 6Cal + $12H_2O$; 8, 2Grs + Cln + $6CO_2$ = 5Prp + 6Cal + $12H_2O$; 9, 3Cln + 5Ms + 24Cal + 15Qtz = 8Grs + 5Phl + $24CO_2$ + $12H_2O$. The left-hand side of each equilibrium corresponds to the low-temperature side of the curves in Figs. 5*a* and 5*c*. For Fig. 5*b*, the topologies can be derived from Figs. 5*a* and 5*c*.

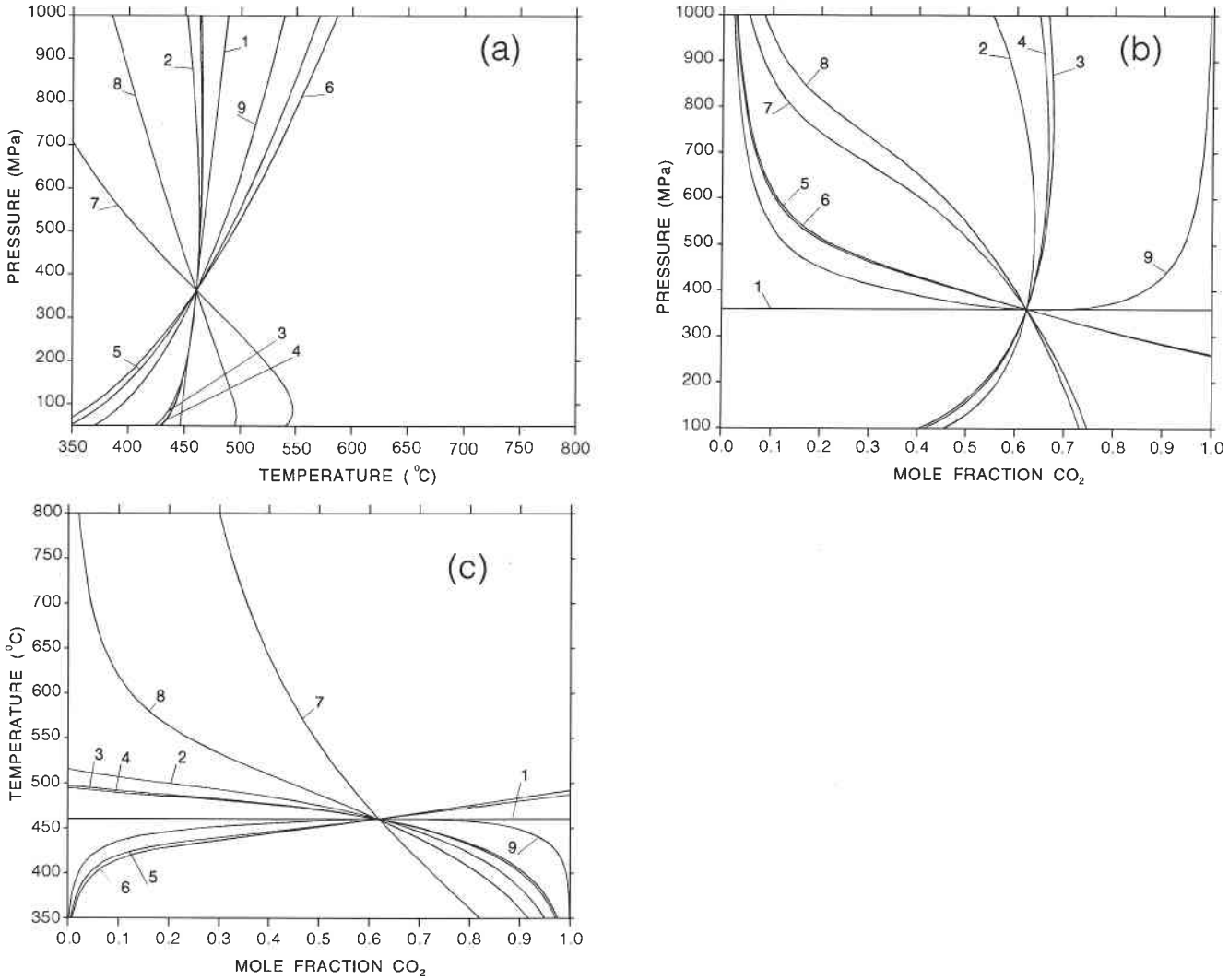

exhausted. In those rocks containing a low modal abundance of relatively Mn-poor garnet, reaction [2] alone may have produced the garnets, whereas in rocks with a higher modal abundance of relatively Mn-rich garnet, reaction [2] may have proceeded either simultaneously with or following completion of reaction [1].

A temperature estimate for the deposit of 450 ± 50°C was made from the average of the five highest estimates, samples S3-11, S7-150, S7-153, DS-47, and DS-85. The uncertainty results from recalculating the equilibrium at two standard deviations of the mineral analyses (Ferry and Spear 1978).

Geobarometry

Among the many different rock types examined from the Sullivan deposit, only one with a mineral assemblage useful for geobarometry was identified, namely sample S3-11 with the mineral assemblage Grt–Bt–Ms–Chl–Cal–Qtz (mineral analyses are given in Table 3). The subassemblage Grt–Pl–Ms–Bt is potentially useful for fluid-independent geobarometry (Ghent and Stout 1981), and was identified in a number of samples. However, the equivocal nature of the plagioclase compositions precluded its use in thermbarometric calculations (see Mineral chemistry section).

Pressure – temperature – fluid composition diagrams for sample S3-11 were generated using TWEEQU computer software (Berman 1988, 1991). Pressure–temperature, pressure–X_{CO_2}, and temperature–X_{CO_2} diagrams for location 2 in sample S3-11 are given in Figs. 5*a*, 5*b*, and 5*c*, respectively. A summary of the P–T–X results from all three locations is given in Table 5.

With the exception of the garnet–biotite Fe–Mg equilib-

Table 5. Temperature, pressure, and fluid-composition estimates from samples S3-11.

Location	Temperature (°C)	Pressure (MPa)	X_{H_2O}
1	470	480	0.44
2	460	360	0.38
3	450	300	0.31
Average	460	380	0.38

rium, equilibria from this assemblage (Grt−Bt−Ms−Chl−Cal−Qtz) involve a fluid phase. These include dehydration equilibria with near-vertical slopes in $P-T$ space (curves 2, 3, and 4 in Fig. 5*a*), decarbonation equilibria with moderate positive slopes in $P-T$ space (curves 5, 6, and 9 in Fig. 5*a*), and carbonation, dehydration equilibria with moderate negative slopes in $P-T$ space (curves 7 and 8 in Fig. 5*a*). The position of the these equilibria in $P-T-X$ space changes as the H_2O/CO_2 ratio of the fluid phase is varied. Without an independent determination of the metamorphic fluid composition, the H_2O/CO_2 ratio that gave the tightest intersection of the equilibrium curves was selected. Because there are only three independent equilibria, the curves can be made to intersect at a point. The high angle of intersection of the equilibrium curves in Fig. 5*b* demonstrates that the H_2O/CO_2 ratio selected need only be varied slightly before the tight intersection is destroyed.

The average pressure estimate between the three locations in sample S3-11 is 380 ± 100 MPa (Table 5). The uncertainty results from recalculating the equilibrium at two standard deviations of the mineral analyses.

Fluid composition

The average of the fluid compositions from the three locations in sample S3-11 is $X_{H_2O} = 0.38$, $X_{CO_2} = 0.62$ (Table 5). This relatively H_2O-poor fluid estimate is particular to the individual sample analyzed, and may not be representative of fluid compositions in all the rocks in the deposit. The deviation of the maximum X_{H_2O} (0.44) and minimum X_{H_2O} (0.31) from the mean X_{H_2O} (0.38) between the three determinations, a value of ±0.07, is taken as an indication of the uncertainty in the fluid composition estimate.

The pressure estimate was calculated assuming the metamorphic fluid was a H_2O-CO_2 binary. An estimate of CO, CH_4, H_2, H_2S, SO_2, and COS concentrations in the fluid phase was made with the computer software of Connolly and Cesare (1993). The determination was made assuming the presence of graphite and the pyrite−pyrrhotite sulphur activity buffer. Although graphite was not observed, and the composition of pyrrhotite was not determined, these conditions were chosen to give the maximum possible concentrations of the trace fluid phases. Table 6 shows that only H_2O and CO_2 would have been present in the fluid phase of this sample in significant concentrations, indicating that the assumption of an H_2O-CO_2 binary fluid is reasonable. C−O−H−S trace species concentrations in a metamorphic fluid do not reach significant concentrations at this grade regardless of the H_2O/CO_2 ratio of the fluid; therefore metamorphic fluids for the deposit as a whole were likely an H_2O-CO_2 binary.

Table 6. Fluid species concentrations for samples S3-11.

Species	Mole fraction
H_2O	0.32
CO_2	0.68
CO	1.25×10^{-4}
CH_4	3.07×10^{-4}
H_2	5.74×10^{-5}
H_2S	1.31×10^{-3}
SO_2	6.22×10^{-10}
COS	3.30×10^{-5}

Notes: Not normalized to 100.0%. X_{H_2O} and X_{CO_2} from TWEEQU software, others from Connolly and Cesare (1993).

Amphibolite equilibria and the age of metamorphism

Several Pb−Pb ages for titanite in the Sullivan area suggest a metamorphic event at ca. 1330 Ma. Ross et al. (1992) obtained an age of 1350 ± 25 Ma for titanite in the Moyie sills south of the Sullivan mine, and Schandl et al. (1993) determined an age of 1320 ± 12 Ma for titanite from chlorite−pyrite alteration in the footwall of the Sullivan deposit.

Titanite in sample S-15 from the metamorphosed gabbro arch on the western edge of the deposit occurs as thin rims on ilmenite (Fig. 2*d*), suggesting a metamorphic origin. An attempt to calculate a unique $P-T$ estimate for this sample using equilibria that involved titanite was unsuccessful, because many potentially useful equilibria could not be used owing to the variable alteration and equivocal compositional variation of plagioclase (see Mineral chemistry section). Moreover, several of the amphibole end members of Mader and Berman (1992) produced erratic and implausible results (i.e., pressures of >1000 MPa at 450°C), most likely because they were derived from natural amphiboles at granulite-facies conditions, far removed from the low-grade conditions of this study. Consequently, the only amphibole end members used were actinolite and tremolite. Despite these problems, a nonunique $P-T$ estimate from this sample from the mineral assemblage Amp−Czo−Chl−Cal−Ilm−Ttn−Qtz (mineral analyses are given in Table 3) provided some constraints on the $P-T$ conditions of metamorphism and, potentially, the age of the metamorphic event.

The $P-T$ diagram for the equilibria from sample S-15 is shown in Fig. 6. Because only two of the five equilibria are independent, the curves will always intersect at a point, and because all five equilibria involve a fluid phase, the position of the intersection changes as the H_2O/CO_2 ratio is varied. As a result, a unique $P-T-X$ determination is not possible. However, the curves can be made to intersect at 480°C and 340 MPa when an X_{H_2O} of 0.60 is chosen (an X_{H_2O} of 0.40 places the intersection at 440°C and 150 MPa, and an X_{H_2O} of 0.80 places the intersection at 520°C and 590 MPa). This is close to the $P-T$ conditions obtained from the metapelitic samples. Given the CO_2-rich composition of the metamorphic fluid in the calcite-bearing metapelite (S3-11),

an X_{H_2O} of 0.60 seems plausible. These results are consistent with textural evidence indicating that titanite in this sample grew during the metamorphic event, and therefore suggest that the titanite ages near 1330 Ma are likely the age of the peak metamorphism.

Discussion

Tectonic significance of $P-T-X$ estimate

The temperature–pressure estimate of this study is consistent with the regional metamorphic grade (biotite zone). A pressure of 380 MPa is equivalent to approximately 14 km of lithostatic load (assuming a rock density of 2.7 g/cm^3). For 450°C, this gives a geothermal gradient of 32°C/km, similar to the average geothermal gradient today of 30°C/km (Best 1982), and, consequently, consistent with burial metamorphism.

The pressure–temperature results of this study (450°C, 380 MPa) together with an age of 1330 Ma for peak metamorphism have tectonic implications for the area. Accounting for 14 km of burial (380 MPa) during peak metamorphism is problematic. There is approximately 7 km of stratigraphy between the Sullivan orebody and the overlying Purcell Lavas (Ethier et al. 1976), which have been dated at 1075 Ma (Hunt 1962). No major unconformities have been identified below the Purcell Lavas. The sediments between the Sullivan orebody and the Purcell Lavas are conformable except for the contact between the Kitchener–Siyeh formation and overlying Purcell Lavas, which is in some places conformable and in others unconformable (Hamilton et al. 1982).

Taking into consideration the uncertainty in the pressure estimate (±100 MPa), a pressure of 480 MPa is equivalent to 18 km of lithostatic load, giving a geothermal gradient of 25°C/km, and a pressure of 280 MPa is equivalent to 10 km of lithostatic load, giving a geothermal gradient of 45°C/km. The higher pressure estimate requires 11 km of erosion below the Purcell Lavas. The lower pressure estimate requires only 3 km of erosion at the unconformity below the Purcell Lavas, but a thermal anomaly would be neccessary to account for the high geothermal gradient. Causes for a thermal anomaly include magmatic intrusions (the nearby Hellroaring Creek stock has been dated at 1260 ± 50 Ma, Ryan and Blenkinsop 1971) or heat produced from a possible Proterozoic orogenic event.

Estimation of metamorphic conditions in metamorphosed ore deposits

The results from this study carry implications for the study of other metamorphosed ore deposits. The advantage of using silicate–carbonate–fluid equilibria from a single experimentally based thermodynamic data base is that $P-T$ conditions in addition to fluid compositions can be determined simultaneously, and the results are internally consistent. This situation contrasts with application of individual equilibria, which do not guarantee internal consistency and, in the case of sulphide equilibria, may be based on poorer quality experimental data. Another reason for favoring the results from silicate–carbonate–fluid equilibria is that silicates may be more retentive of peak metamorphic compositions compared with some sulphides; for example, sphalerite often shows evidence for resetting, resulting in too high pressure estimates, whereas diffusion rates in silicates at low-grade conditions such as at Sullivan are slow enough that retention of prograde or peak metamorphic compositions is likely. This situation may not apply under higher grade conditions (see below).

Fig. 6. Pressure–temperature diagram for sample S-15. X_{H_2O} of diagram = 0.60. Mineral assemblage is Amp–Czo–Chl–Cal–Ilm–Ttn–Qtz. Two independent reactions. Intersection temperature = 480°C; pressure = 340 MPa. Assemblages on the left are stable on the low-temperature side of equilibrium. 1, 21Act + 105Ttn + 39Cln + 17CO_2 = 17Cal + 105Ilm + 39Tr + 26Czo + 125H_2O; 2, 10Act + 50Ttn + 17Qtz + 21Cln = 50Ilm + 21Tr + 14Czo + 66H_2O; 3, 21Qtz + 3Cln + 10Cal = 3Tr + 2Czo + 10CO_2 + 8H_2O; 4, 125Qtz + 40Ilm + 3Cln + 66Cal = 40Ttn + 3Tr + 8Act + 2Czo + 66CO_2; 5, 13Qtz + 5Ilm + 7Cal + H_2O = 5Ttn + Act + 7CO_2.

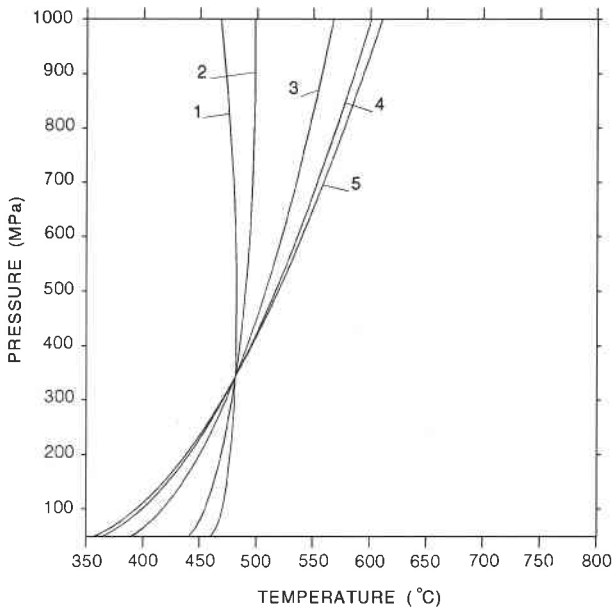

Estimation of metamorphic conditions in low-grade rocks

The results of this study also carry implications for the interpretation of $P-T$ results of metamorphic rocks in general. Our interpretation of mineral compositions and resulting temperatures at Sullivan provides an interesting contrast to temperature estimation in high-grade rocks such as granulites. In granulites, diffusion rates are fast enough that differential reequilibration of cations during cooling from peak conditions invalidates the equilibrium assumption required for multiequilibrium thermobarometry (Pattison and Bégin 1994), and makes temperature estimation problematic. In contrast, at low grades, diffusion rates are so slow that equilibration can probably only proceed by recrystallization in the presence of a fluid medium. Consequently, if some minerals, such as garnet, cease to grow prior to the attainment of peak conditions, they may retain their compositions from the earlier prograde part of the metamorphic event. If other minerals in the rock, especially those with

faster cationic diffusivities such as sheet silicate minerals, continue to wholly or partially equilibrate up to peak metamorphic conditions, the problem of disequilibrium between garnet and the other minerals arises. Thus, as for granulites, the equilibrium assumption is compromised. It may be that there is only a fairly small range of grade (approximately mid-amphibolite grade) in which diffusion is fast enough to allow mineral compositions to equilibrate as temperature rises and yet slow enough to preserve the peak compositions during cooling.

In our study of low-grade metamorphic rocks at Sullivan, analysis of the mineral assemblages and inferred reaction history of the different rocks allowed qualitative inferences to be made about when certain minerals (particularly garnet) may have stopped growing in different rocks. These considerations appeared to provide the best explanation for the observed temperature scatter. This technique may have application to other low-grade metamorphic settings.

Conclusions

The Sullivan orebody has been metamorphosed to transitional greenschist–amphibolite facies. Mineral textures in the deposit are metamorphic. The orebody contains abundant metamorphic garnet, in contrast to the lower grade Bt–Chl regional assemblage outside of the deposit. The presence of garnet within the deposit is likely due to more Mn-rich bulk compositions within the orebody as compared with the surrounding sediments. Peak metamorphic temperature as determined by the Berman (1990) calibration of the garnet–biotite Fe–Mg exchange equilibrium is 450 ± 50°C. Lower temperature estimates from some samples are interpreted to record the temperature of cessation of garnet growth prior to peak metamorphic conditions. Peak metamorphic pressure as determined from the assemblage Grt–Bt–Ms–Chl–Cal–Qtz is 380 ± 100 MPa. The fluid composition required for this estimate is $X_{H_2O} = 0.38$, $X_{CO_2} = 0.62 \pm 0.07$. This fluid composition is specific to one sample and may not be representative of fluid compositions in all the rocks in the deposit. Metamorphic fluids in the deposit were essentially a H_2O–CO_2 binary. Both textural evidence and P–T results obtained from a sample of a metamorphosed mafic intrusion in the deposit are consistent with the conclusion that titanite ages near 1330 Ma obtained in the Sullivan mine area are the age of the peak metamorphic event. The results of this study carry implications for the regional tectonic history of the Sullivan area, as well as implications for determining metamorphic conditions in ore deposits and low-grade metamorphic rocks in general.

Acknowledgments

Funding for this work was provided by the Natural Sciences and Engineering Research Council of Canada grant 037233 to D.R.M.P. The authors wish to thank Dr. Fin Campbell for making available the suite of Sullivan mine samples, and Dr. N.J. Begin and Dr. W. Powell for reviewing an early version of the manuscript. We thank journal reviewers Dr. G. Dipple and G. Skippen for their comments, which improved the presentation of this paper.

References

Bachinski, J.R. 1976. Metamorphism of cuperiferous iron deposits, Notre Dame Bay, Newfoundland. Economic Geology, **71**: 443–452.

Begin, N.J. 1992. Contrasting mineral isograd sequences in metabasites of the Cape Smith Belt, northern Quebec, Canada: three new bathograds for mafic rocks. Journal of Metamorphic Geology, **10**: 685–704.

Benvenuto, G.L., and Price, R.A. 1979. Structural evolution of the Hosmer thrust sheet, southeastern British Columbia. Bulletin of Canadian Petroleum Geology, **27**: 360–394.

Berman, R.G. 1988. Internally-consistent thermodynamic data for stoichiometric minerals in the system Na_2O–K_2O–CaO–MgO–FeO–Fe_2O_3–Al_2O_3–TiO_2–H_2O–CO_2. Journal of Petrology, **29**: 445–522.

Berman, R.G. 1990. Mixing properties of Ca–Mg–Fe–Mn garnets. American Mineralogist, **75**: 328–344.

Berman, R.G. 1991. Thermobarometry using multiequilibrium calculations: a new technique with petrological applications. Canadian Mineralogist, **29**: 833–855.

Best, M.G. 1982. Igneous and metamorphic petrology. W.H. Freeman and Company, New York, San Francisco.

Campbell, F.A., and Ethier, V.G. 1983. Environment of deposition of the Sullivan orebody. Mineralium Deposita, **18**: 39–55.

Chakraborty, S., and Ganguly, J. 1991. Compositional zoning and cation diffusion in garnet. *In* Diffusion, atomic ordering, and mass transport. Advances in physical geochemistry. Vol. 8. *Edited by* J. Ganguly. Springer Verlag, New York, pp. 120–175.

Chatterjee, N.D., and Froese, E.F. 1975. A thermodynamic study of the pseudobinary join muscovite–paragonite in the system $KAlSi_3O_8$–$NaAlSi_3O_8$–Al_2O_3–SiO_2–H_2O. American Mineralogist, **60**: 985–993.

Chipera, S.J., and Perkins, D. 1988. Evaluation of biotite–garnet geothermometers: application to the English River subprovince, Ontario. Contributions to Mineralogy and Petrology, **98**: 40–48.

Connolly, J.A.D., and Cesare, B. 1993. C–O–H–S fluid compositions and oxygen fugaity in graphitic metapelites. Journal of Metamorphic Geology, **11**: 379–388.

De Paoli, G.R. 1994. Metamorphism of the Sullivan orebody, Kimberley, British Columbia, using silicate–carbonate equilibria. M.Sc. thesis, The University of Calgary, Calgary, Alta.

Droop, G.T.R. 1985. Alpine metamorphism in the south-east Tauern Window, Austria. 1. P–T variations in space and time. Journal of Metamorphic Geology, **3**: 371–402.

El-Shazly, A.K., and Liou, J.G. 1991. Glaucophane chloritoid-bearing assemblages from NE Oman: petrologic significance and a petrogenetic grid for high P/T metapelites. Contributions to Mineralogy and Petrology, **107**: 180–201.

Ethier, V.G., Campbell, F.A., Both, T.A., and Krouse, H.R. 1976. Geological setting of the Sullivan orebody and estimates of temperatures and pressure of metamorphism. Economic Geology, **71**: 1570–1588.

Ferry, J.M., and Spear, F.S. 1978. Experimental calibration of the partitioning of Fe and Mg between biotite and garnet. Contributions to Mineralogy and Petrology, **66**: 113–117.

Froese, E. 1969. Metamorphic rocks from the Coronation mine and surrounding area. Geological Survey of Canada, Paper 68-5, pp. 55–77.

Ghent, E.D., and Stout, M.Z. 1981. Geobarometry and geothermometry of plagioclase–biotite–garnet–muscovite assemblages. Contributions to Mineralogy and Petrology, **76**: 92–97.

Hamilton, J.M., Bishop, D.T., Morris, H.C., and Owens, O.E. 1982. Geology of the Sullivan orebody, Kimberley, B.C.,

Canada. *In* Precambrian sulphide deposits, H.S. Robinson memorial volume. *Edited by* R.W. Hutchinson, C.D. Spence, and J.M. Franklin. Geological Association of Canada, Special Paper 25, pp. 598–680.

Hodges, K.V., and Spear, F.S. 1982. Geothermometry, geobarometry and the Al_2SiO_5 triple point at Mt. Moosilauke, New Hampshire. American Mineralogist, **67**: 1118–1134.

Hunt, G. 1962. Time of Purcell eruption in southeastern British Columbia and southwestern Alberta. Journal of the Alberta Society of Petroleum Geologists, **10**: 438–442.

Hutcheon, I. 1979. Sulphide–oxide–silicate equilibria; Snow Lake, Manitoba. American Journal of Science, **279**: 643–665.

Kretz, R. 1983. Symbols for rock-forming minerals. American Mineralogist, **68**: 277–279.

Kretchmar, U., and Scott, S.D. 1976. Phase relations involving arsenopyrite in the system Fe–As–S and their applications. Canadian Mineralogist, **14**: 364–386.

LeCouter, P.C. 1973. A study of lead isotopes from mineral deposits in southeastern British Columbia and the Anvil Range, Yukon Territory. Ph.D. thesis, The University of British Columbia, Vancouver.

Leitch, C.H.B. 1991. Preliminary fluid inclusion and petrographic studies of parts of the Sullivan stratiform sediment-hosted Pb–Zn deposit, southeastern British Columbia. *In* Current research, part A. Geological Survey of Canada, Paper 91-1A, pp. 91–101.

Leitch, C.H.B., and Turner, J.W. 1992. The vent complex of the Sullivan stratiform sediment-hosted Zn–Pb deposit, British Columbia: preliminary petrographic and fluid inclusion studies. *In* Current research, part E. Geological Survey of Canada, Paper 91-1E, pp. 33–44.

Lis, M.G., and Price, R.A. 1976. Large-scale block faulting during deposition of the Windermere Supergroup (Hadrynian) in southeastern British Columbia. *In* Current research, part A. Geological Survey of Canada, Paper 76-1A, pp. 135–136.

Lydon, J., Hoy, T., and Turner, R. 1995. Special session on: Continental rifting and the formation of sedex deposits: Sullivan and other giants. Geological Association of Canada, Programs and Abstracts, **20**: 12–13, 18.

Mader, U.K., and Berman, R.G. 1992. Amphibole thermobarometry: a thermodynamic approach. *In* Current research, part E. Geological Survey of Canada, Paper 92-1E, pp. 393–400.

Maruyama, S., Liou, L.G., and Suzuki, K. 1982. The peristerite gap in low-grade metamorphic rocks. Contributions to Mineralogy and Petrology, **81**: 268–276.

McMechan, M.E., and Price, R.A. 1982. Superimposed low-grade metamorphism in the Mount Fisher area, southeastern British Columbia — implications for the East Kootenay orogeny. Canadian Journal of Earth Sciences, **19**: 476–489.

McMullin, D.W.A., Berman, R.G., and Greenwood, H.J. 1991. Calibration of the SGAM thermobarometer for pelitic rocks using data from phase-equilibrium experiments and natural assemblages. Canadian Mineralogist, **29**: 889–908.

Nesbitt, B.E. 1982. Metamorphic sulphide–silicate equilibrium in the massive sulphide deposits at Ducktown, Tennessee. Economic Geology, **77**: 364–378.

Nicholls, J., Fiesenger, D.W., and Ethier, V.G. 1977. FORTRAN programs for processing routine electron microprobe data. Computers and Geosciences, **3**: 49–83.

Pattison, D.R.M., and Bégin, N.J. 1994. Zoning patterns in orthopyroxene and garnet in granulites: implications for geothermometry. Journal of Metamorphic Geology, **12**: 387–410.

Raeside, P.R., Hill, J.D., and Eddy, B.G. 1988. Metamorphism of Meguma Group metasedimentary rocks, Whitehead Harbour area, Guysborough County, Nova Scotia. Maritime Sediments and Atlantic Geology, **24**: 1–9.

Read, P.B., Woodsworth, G.J., Greenwood, H.J., Ghent, E.D., and Evenchick, C.A. 1991. Metamorphic map of the Canadian Cordillera. Geological Survey of Canada, Map 1714A.

Ross, G.M., Parrish, R.R., and Winston, D. 1992. Provenance and U–Pb geochronology of the Mesoproterozoic Belt Supergroup (northwestern United States): implications for the age of deposition and pre-Panthalassa plate reconstructions. Earth and Planetary Science Letters, **113**: 57–76.

Ryan, B.D., and Blenkinsop, J. 1971. Geology and geochronology of the Hellroaring Creek Stock, British Columbia. Canadian Journal of Earth Sciences, **8**: 85–95.

Schandl, E.S., Davis, D.W., and Gorton, M.P. 1993. The Pb–Pb age of metamorphic titanite in the chlorite–pyrite altered footwall of the Sullivan Zn–Pb SEDEX deposit, B.C., and its relationship to the ore. *In* Program and Abstracts, Geological Association of Canada – Mineralogical Association of Canada, Joint Annual Meeting, 1993, p. A93.

Scott, S.D. 1973. Experimental calibration of the sphalerite geobarometer. Economic Geology, **68**: 446–474.

Spear, F.S. 1991. On the interpretation of peak metamorphic temperature in light of garnet diffusion during cooling. Journal of Metamorphic Geology, **9**: 379–388.

Symmes, G.H., and Ferry, J.M. 1992. The effect of whole-rock MnO content on the stability of garnet in pelitic schists during metamorphism. Journal of Metamorphic Geology, **10**: 221–237.

Walther, J.V., and Wood, B.J. 1984. Rate mechanisms in prograde metamorphism. Contributions to Mineralogy and Petrology, **88**: 246–259.

Wood, B.J., and Walther, J.V. 1983. Rates of hydrothermal reactions. Science (Washington, D.C.), **222**: 413–415.